USE OF CAPNOGRAPHY TO VERIFY EMERGENCY VENTILATOR SHARING IN THE COVID-19 ERA

Anita Korsós MD[1], Ferenc Peták PhD, DSc[2], Roberta Südy MD[1], Álmos Schranc MD[2], Gergely H. Fodor MD, PhD[2], Barna Babik MD, PhD[1]

[1] Department of Anaesthesiology and Intensive Therapy, University of Szeged, 6 Semmelweis Street, H 6725 Szeged, Hungary

[2] Department of Medical Physics and Informatics, University of Szeged, 9 Koranyi fasor, H 6720 Szeged, Hungary

Running head: Emergency ventilator sharing with capnography

Address for correspondence:

Ferenc Peták

Department of Medical Physics and Informatics

University of Szeged

9 Korányi fasor, H-6720, Szeged, Hungary

Email: petak.ferenc@med.u-szeged.hu

Phone/Fax: +36 62 545832

ABSTRACT

Exacerbation of COVID-19 pandemic may lead to acute shortage of ventilators, which may require shared use of ventilator as a lifesaving concept. Two model lungs were ventilated with one ventilator to i) test the adequacy of individual tidal volumes via capnography, ii) assess cross-breathing between lungs, and iii) offer a simulation-based algorithm for ensuring equal tidal volumes. Ventilation asymmetry was induced by placing rubber band around one model lung, and the uneven distribution of tidal volumes (VT) was counterbalanced by elevating airflow resistance (HR) contralaterally. VT, end-tidal CO_2 concentration ($ETCO_2$), and peak inspiratory pressure (Ppi) were measured. Unilateral LC reduced VT and elevated $ETCO_2$ on the affected side. Under HR, VT and $ETCO_2$ were re-equilibrated. In conclusion, capnography serves as simple, bedside method for controlling the adequacy of split ventilation in each patient. No collateral gas flow was observed between the two lungs with different time constants. Ventilator sharing may play a role in emergency situations.

Keywords: COVID-19, pandemic, mechanical ventilation, ventilator splitting, capnography, respiratory mechanics, lung compliance, respiratory resistance, respiratory rescue manoeuvre

1. INTRODUCTION

At the beginning of 2020 the newly emerged SARS-CoV-2 virus caused a worldwide outbreak referred to as the COVID-19 pandemic. This new coronavirus may cause viral pneumonia with severe respiratory insufficiency requiring mechanical ventilation in up to 17-19% of the hospitalized cases (Lee et al., 2020; Zhou et al., 2020). The need for ventilatory support at any critical moment is influenced by various factors. First, the virus spreads quickly in the community causing a rapid rise in the number of infected patients in a relatively short timeframe (Noble et al., 2020; Park et al., 2020; Sanche et al., 2020). Secondly, as critical care physicians become more familiar with the detrimental course of the COVID-19, expert opinions and consensus statements suggest to initiate invasive ventilation as early as possible after escalation of respiratory symptoms (Brochard et al., 2017; Gattinoni et al., 2020; Marini and Gattinoni, 2020; Wax and Christian, 2020; Wilcox, 2020). Finally, most patients requiring mechanical ventilation generally depend on these ventilators for a prolonged period of time, which may last up to 14 days (Bhatraju et al., 2020; Chen et al., 2020). Under extreme circumstances, these factors may lead to a need for a high number of mechanical ventilators to meet the demand for the simultanous life support.

However, the increased need for ventilators is transient, ventilatory equipments are expensive and their immediate manufacturing is proven to be difficult. Therefore, the supply is limited by economic and technical factors that may lead to a scenario when intensivists are bound to rely on the the number of available ventilators in their units. Hence, the actual need for ventilators may exceed the number of available devices in case of a severe regional outbreak of COVID-19 in low- and even in high-income countries (Beitler et al., 2020). This may lead to an inevitable triage, with quick and difficult decision making necessary regarding the rational utilisation of critical care based on promptly available information (Shovlin and Vizcaychipi, 2020). Ultimately, this raises ethical concerns, as the chance of survival of patients with severe

respiratory insufficiency without mechanical ventilation is unquestionably lower in the presence of viral pneumonia. Therefore it is reasonable not to dismiss the concept of ventilator sharing as a life saving maneuver, which means ventilating multiple lungs of similar patients with one apparatus. This rescue option may have importance in a second wave of the COVID-19 pandemic and/or in low-income countries with limited resources in their health care systems. This emergency approach has been previously described (Chatburn et al., 2020; Clarke et al., 2020; Herrmann et al., 2020; Kheyfets et al., 2020; Neyman and Irvin, 2006; Paladino et al., 2008) and more recently its feasibility was confirmed in experiemntal (Kheyfets et al., 2020) and bench-test studies (Chatburn et al., 2020; Clarke et al., 2020; Herrmann et al., 2020; Kheyfets et al., 2020). While these previous studies focused on the equal distribution of tidal volumes, balancing tidal volumes does not guarantee adequate ventilation on both sides if patients differ in their metabolic rates. Capnography as a simple, routine monitoring modality takes into account the balance of the demand and supply and it is helpful to verify the adequacy of ventilation in both individuals. However, many potential issues need clarification before considering this approach in clinical situations. Of these, the present experimental bench-test study aims at i) testing the use of capnography as a simple, noninvasive, online and goal-oriented bedside method for contolling the adequacy of shared ventilation in each patients, ii) investigating the presence of potential collateral gas flow between the two lungs with different time constants, and iii) offering a simulation-based algorithm for ensuring equal tidal volumes by counterbalancing the difference in compliances by adjusting the resistance on the contralateral side.

2. METHODS

2.1. The experimental setup

The experimental setup is shown schematically in Figure 1. Testing apparatus included two symmetrical model lungs. The model on each side was built from a 7-mm inner diameter commercial endotracheal tube to mimic the airways, and a commercially available artificial lung (type VA8001, Great Group Medical Co., Ltd., Taiwan) to represent compliant respiratory tissues. This double-lung system was ventilated with a commercially used ventilator (Dräger Evita XL, Dräger Medical, Lübeck, Germany). The ventilator circuit was divided symmetrically into two inspiratory and expiratory limbs with lengths of 110 cm, by introducing Y-piece connectors close to the inlet and outlet ports of the ventilator. Both inspiratory and expiratory tubing were connected after the inspiratory and before the expiratory valves of the respirator, respectively. While this approach is the most simple and clear scenario in emergency clinical environment, it raises the possibility of cross-breathing between the two lungs.

Two mainstream capnographs (Capnogard 1265, Novametrix, Andover, MA, USA) were connected to each circuit to estimate pendelluft between the two lung models. The airflow (V') on each side was measured by a 11-mm internal diameter pneumotachograph (PNT Series, Hans Rudolph, Shawnee, KS, USA) connected to a miniature differential pressure transducer (24PCE-FA6D Honeywell, Charlotte, NC, USA). The pressure inside each model lung respectively was measured via connecting identical pressure sensors (24PCE-FA6D Honeywell, Charlotte, NC, USA) to the lateral ports. A rubber band was used on one side referred as Low C to decrease the compliance, whereas a Hoffmann clamp was placed around the endotracheal tube on the contralateral side referred as High R.

Plastic tubing was attached to the apex of each test lung allowing a carbon dioxide (CO_2) gas inflow from a CO_2 reservoir bag supplied by a medical CO_2 cylinder. To ensure identical

amount of CO_2 delivery into each side, a roller pump (Terumo Sarns 9000 Heart-Lung Machine, Terumo Europe NV, Leuven Belgium) was used as a flow generator to feed the CO_2 tubing system divided with a T-piece. To avoid uneven distribution of CO_2 flow into each lung side depending on the load impedance, each tubing used to deliver CO_2 was equipped with an on-off clamp, which allowed delivering CO_2 into one side only during the capnography measurements. This system guaranteed the delivery of the same CO_2 concentration alternately even if the impedance of the artificial lung is varied depending on the applied elastic and/or resistive load. This setup mimics physiological CO_2 production with a constant rate of 200 ml/min. The CO_2 delivery system also enabled monitoring of the adequacy of ventilation via measuring the end-tidal partial pressure of CO_2 ($ETCO_2$) on each side, respectively. In addition, unilateral CO_2 delivery combined with bilateral capnography allows the assessment of the potential collateral gas flow between the two lungs with different time constants.

2.2. Data acquisition

Data epochs containing 30-s registrations of airflow and pressure signals of each test lung were digitized at a sampling rate of 256 Hz and recorded via a custom-made data acquisition software. The time-series datasets were analysed by using the LabChart software (version 7, ADInstruments, Sydney, Australia). The peak inspiratory (PIF) and expiratory flow rates (PEF), and the peak inspiratory pressure (Ppi) were determined via peak analyses. Tidal volumes (VT) for each lung were calculated by integrating the corresponding V' signals. Respiratory parameters characterising both lungs together were registered from the display of the respirator. Values of VT, PIF, PEF, Ppi and $ETCO_2$ were averaged over the 30-s measurement period; since the bench test results were highly reproducible, the scatters in the parameters were negligible (coefficient of variation <0.7%).

2.3. Simulation study

A mathematical simulation study was performed to assess the magnitude of the resistance required to counterbalance the decreased compliance on the contralateral side, to meet the clinical need of delivering equal tidal volumes to both patients connected to the shared ventilation circuit. The simulation was based on the postulation that equal tidal volumes are delivered to both lungs if the absolute values of the loading impedances are identical, even if the resistive and elastic components are different on the two sides:

$$|Z_{LC}| = |Z_{HR}| \quad (1)$$

Indexes LC and HR refer to low compliance (Low C) and high resistance (High R) lung sides, respectively. The total respiratory impedance in the range of normal ventilation contains a real part (R) representing the resistive, and an imaginary part (X) reflecting the elastic components. Considering that the absolute value of an impedance is calculated as $Z = \sqrt{R^2 + X^2}$, equation (1) can be written as:

$$\sqrt{R_{LC}^2 + X_{LC}^2} = \sqrt{R_{HR}^2 + X_{HR}^2} \quad (2)$$

We modelled the respiratory system impedance with two parallel single compartment models (Fig. 1A). In this frequency domain impedance model, the real parts can be represented by single resistance values (R_{LC} and R_{HR}), while the X is inversely related to compliance ($X=1/(2\pi fC)$), where f is the ventilation frequency). Accordingly, equation 2 is written as:

$$\sqrt{R_{LC}^2 + \left(\frac{1}{2\pi f C_{LC}}\right)^2} = \sqrt{R_{HR}^2 + \left(\frac{1}{2\pi f C_{HR}}\right)^2} \quad (3)$$

Rearranging equation 3 yields that the resistance needed to counterbalance the decreased compliance on the contralateral side can be expressed as:

$$R_{HR} = \sqrt{R_{LC}^2 + \left(\frac{1}{2\pi f C_{LC}}\right)^2 - \left(\frac{1}{2\pi f C_{HR}}\right)^2} \quad (4)$$

The initial values of the resistance and compliance parameters were based previously established values typical for mechanically ventilated adults with healthy lungs (Babik et al., 2002). The resistance on the high-resistance side (R_{HR}) was calculated by setting the airway resistance value of 8 $cmH_2O.s/l$ for the lung side with low compliance (R_{LC}), and identical lung compliances for each side of 80 ml/cmH_2O (C_{LC} and C_{HR}) by using equation (4). Unilateral decrease in lung compliance was simulated thereafter with keeping R_{LC} and C_{HR} constant with original values of 8 $cmH_2O.s/l$ and 80 ml/cmH_2O, respectively, while C_{LC} was decreased stepwise from 80 to 20 ml/cmH_2O. Equation (4) was used to calculate the R_{HR} values needed to compensate these asymmetries to equilibrate the differences in the absolute values of the mechanical impedances. Stepwise decreases in C_{HR} were then considered until 30 ml/cmH_2O, and the values of the corresponding C_{LC} were calculated in an identical manner. The compliance was considered highly variable between two simulated patients, since virus pneumonia in COVID-19 compromises primarily the lung distensibility (Gattinoni et al., 2020; Marini and Gattinoni, 2020). Finally, the same simulation procedure was repeated when a moderately elevated total respiratory resistance was considered on the low compliance lung side (R_{LC} = 12 $cmH_2O.s/l$); this value was also based on the values typical for mechanically ventilated adults with moderate obstruction (Babik et al., 2002).

Ventilation parameters (e.g. ventilation mode, PEEP, respiratory I:E ratio) affect resistance and compliance values used in the simulation study (Grinnan and Truwit, 2005). Thus, resistance and compliance used in our simulation study take into account the ventilator settings on the simulation outcomes.

2.4. Measurement protocol

The first set of data were collected in a system with intact test lungs possessing identical compliance and resistance parameters. Under this baseline condition (BL), volume-control mode with decelerating flow (Draeger Autoflow®) was applied with a total VT of 840 ml divided into 420 ml on each side. The ventilation frequency was 12/min with I:E ratio of 1:2 throughout the study period. The end-expiratory pressure (PEEP) was set to 5 cmH_2O and the resulting Ppi was 22 cmH_2O. Mechanical parameters of ventilation (VT, PIF, PEF and Ppi) were measured in parallel for each lung side. $ETCO_2$ values were registered alternately in each lung by clamping the contralateral limb of CO_2 tubing to avoid shunting of CO_2 delivery to the lung side with lower loading impedance. After completing these baseline measurements, the compliance was compromised with placing the elastic rubber band around one of the test lungs. In this unilateral low-compliance condition (LC), the same measurements were carried out as in condition BL. To counterbalance the decreased compliance on the low compliance side, the resistance was then adjusted with the Hoffmann clamp on the opposite high resistance side, and the same measurement sequence was repeated in this high-resistance condition (HR) as in the BL stage.

The ventilation was then changed to pressure-controlled mode. The pressure control level was set to maintain the same VT as in the volume-control mode, i.e. 22 cmH_2O. Another set of BL data with symmetrical lungs and under Low C condition were then collected identical to the volume-control mode. In the third phase of the measurement when high compliance on one side was associated with high resistance on the other side, the pressure control level was elevated to 29 cmH_2O to provide physiological VT and $ETCO_2$ in both model lungs.

3. RESULTS

Table 1 summarizes the resistance and compliance parameters displayed by the ventilator during the measurements in volume- (VC) and pressure-controlled (PC) ventilation modes, and the calculated time constant ($\tau = R \cdot C$). Readings were made under baseline conditions (BL), after unilateral decrease in compliance (LC) and contralateral compensation with high resistance (LC + HR). To assess the level of asymmetry in the mechanical parameters, individual compliance values were calculated by using the measured individual tidal volumes and distending pressures on each side. Estimation of individual resistances characterizing each side were based on equation (4).

Representative volume, capnogram, airflow and pressure curves are illustrated on Figure 2. Under baseline conditions, the curves obtained on the two lung sides overlap, indicating no difference in the mechanical properties between the two test lungs. After compromising the compliance unilaterally (condition LC), the reduced VT on the stiffer lung side was associated with an increased VT on the other side without intervention. Consequently, the $ETCO_2$ became higher in the lung with low compliance and reduced on the reference side. Following the contralateral elevation of resistance, the VT and $ETCO_2$ values were re-equilibrated, whereas the flow pattern exhibited marked differences with restrictive and obstructive flow patterns on the Low C and High R sides, respectively. The plateau pressure levels elevated stepwise after each intervention, with no difference between the two communicating sides.

The average values of the main outcome parameters are summarized on Figure 3. Under baseline conditions (BL), the VT was equally distributed between the two model lungs, with no difference between the capnography and mechanical parameters both in volume- and pressure-control modes. The unilateral decrease in compliance in volume control mode resulted in an uneven distribution of VTs with lower volume on the interventional side and elevated VT on

the intact model lung. These volume differences were also manifested in the $ETCO_2$ asymmetry. The decrease in global compliance caused elevations in Ppi equally on both sides. Unilateral stiffening during pressure-control ventilation decreased VT and increased $ETCO_2$ on the restricted side, whereas the intact side remained at the baseline level determined by the constant driving pressure level. Counterbalancing the lung restriction contralaterally with an increased flow resistance redirected the ventilation to the stiffer lung. This intervention led to different airflow profiles between the two sides (PIF, PEF) redistributing the mechanical ventilation as evidenced by the normalized VT and $ETCO_2$ levels on both sides. These effects are uniform in volume- and pressure-controlled ventilation modes, however the Ppi needed to be increased intentionally in pressure-controlled mode.

The results of the mathematical simulation study are demonstrated on Figure 4 by assuming normal (left) and elevated (right) total respiratory resistance levels on the low-compliance side. The graphs show the resistance values necessary to counterbalance the asymmetry in compliance values, to therefore deliver the same tidal volumes to both patients connected to the shared ventilation circuit. The compliance values of the two ventilated sides are indicated on the labelled curves and the x-axes, and the targeted contralateral resistance values can be read on the y-axes.

4. DISCUSSION

Due to the high reproduction number of SARS-CoV-2 virus, there may be a sudden increase in the number of patients requiring mechanical ventilation (Park et al., 2020; Sanche et al., 2020). This can lead to an acute shortage of ventilators even in high-income countries with limited health care resources (Beitler et al., 2020) or in case of a second wave of the pandemic. We used capnogaphy in the present study to demonstrate the adequacy of the shared ventillation with no collateral airflow between the split sides, even in case of great differences in their

mechanical load. We also performed a simulation study to recommend contralateral resistance values, which may orient critical care providers to counterbalance a wide range of differences in individual compliances.

In an outbreak, clinicians may be faced with difficult decision making. A triage resulting from the mismatch of patients requiring mechanical ventilation and the number of ventilators currently available is an example of this (Carenzo et al., 2020; Phua et al., 2020; Xie et al., 2020). As an alternative, it is reasonable to propose the concept of ventilator sharing as a lifesaving modality.

Clinical implementation of our setting necessitates components otherwise available in intensive care units. A Hoffmann clamp can be placed over the outer end of the endotrahcheal tube just before the Y-piece. This clamp can be used to gradually decrease the diameter of the ET-tube on the side where the compliance is higher. The other essential component is a capnograph inserted on both sides. This simple and routine monitoring modality will help to guide and control the measure of clench exerted by the Hoffmann clamp until the $ETCO_2$ levels on each side approach each other in the normal range. However, the practical implementation of our concept recommends the use of muscle relaxant to avoid active breathing movements to exclude the potential cross-breathing.

However, ventilator sharing between two patients raises several concerns needing clarification before considering this approach in clinical settings. An important challenge is related to the fact that the simultaneously ventilated individuals may differ in their respiratory mechanics, due to the asymmetry in anthropologic features and/or severity of respiratory symptoms. Given the fact that individual tidal volumes are distributed equally if the magnitude of the input impedances are equal, we offered a quick simulation-based algorithm for ensuring equal tidal volumes by overcoming differences in respiratory mechanics.

It is important to note, however, that the patients may differ in their metabolic rates and diffusion capacities. Thus, equal distribution of tidal volumes does not guarantee adequate ventilation on both sides. Consequently, an additional monitoring modality is mandatory to verify the adequacy of ventilation in both individuals. Therefore, we implemented capnography as a simple, non-invasive, online and bedside method for controlling the adequacy of ventilation (Abid et al., 2017; Balogh et al., 2016). Since expiratory capnogram reflects alveolar ventilation, capillary gas diffusion and lung perfusion, this monitoring tool allows the assessment of the adequacy of ventilation individually in a goal-oriented manner (Csorba et al., 2016). Indeed, the results of the present study confirmed that diminished VT resulting from mechanical asymmetry was associated with hypercapnia in the low compliance side. This can be attributed to the maintained CO_2 production into a smaller gas compartment. Our findings demonstrate that capnography serves as a safe control modality to individualize the redirection of VT into the stiffer side. Since the use of capnography is useful to detect diminished $ETCO_2$ as a prerequisite of lung overinflation, this monitoring modality may also help to prevent volutrauma. However, it should also be noted that low $ETCO_2$ may not reflect high tidal volume in the presence of lung injury due to the compromised gas exchange.

Ventilation with circuit splitting may generate a further concern related to the potential collateral bias flow between the patients. However, the pressure regimen during the ventilation cycle did not differ between the two sides independent of the ventilation mode. The lack of difference in the driving pressure at any time of point of expiration rules out the presence of collateral gas flow. The cross-breathing can also be excluded by the capnography findings, i.e., there was no detectable CO_2 in one lung side when the CO_2 inflow was driven only into the other lung.

The compliance values of the model lungs with baseline compliance values of 27 ml/cmH_2O used in the current bench-test mimic diseased lungs with restricted by viral pneumonia. When

asymmetry was generated, the differences in the compliance values were almost two times. This condition resembles a shared ventilation of a moderately and a severely injured lung. Redirection of airflow by increasing resistance on the higher compliance side compromised lung emptying indicated by the distortion of the expiratory flow curve (Fig 2, LC+HR column, blue line). After the application of this mechanical load, the flow pattern just approaches zero by the end expirations. Further need of such a compensation in resistance may evoke incomplete lung emptying and thereby inducing auto-PEEP and dynamic hyperinflation on the high-compliance high-resistance side, which points to the limitation of the volume-shifting methodology by unilateral resistance manipulation. The substantial increase in τ_{HR} clearly indicates the limits of this approach, since the rate of lung emptying on the HR side decreased significantly in the current experiments (Table 1).

The results of the present study also reveal the differences between the volume- and pressure-controlled ventilation modes to optimize ventilation parameters in a shared system. In case of volume-controlled ventilation, the opposite changes in VT and $ETCO_2$ were observed between the two sides. However, using the pressure-controlled mode affected only the manipulated side. It should be noted that the pressure-control level determining the Ppi has to be elevated to counteract the resistive load used to shift VT into the stiff side (Fig. 3, Ppi).

The limitations of the present study also warrant discussion. For simplicity, in the mathematical simulation study, we considered close to normal or moderately elevated initial resistance values uniformly on both sides. As COVID-19 induces mainly restrictive changes indicated by moderately and severely compromised compliances (Gattinoni et al., 2020; Marini and Gattinoni, 2020), asymmetry was generated in this mechanical parameter. A further simplification of the simulation model was related to the negligence of the dissipative energy loss in the respiratory tissues (Babik et al., 2002), which is expected to be elevated in this pathology. However, there is no data available currently to estimate the magnitude of alterations

in this mechanical parameter. The results of the simulations even with these simplifications can serve as a starting point and the appropriateness of ventilation in each individual can be verified by capnography. Another limitation is related to the target-oriented model, which does not mimic all aspects of ARDS. However, application of the restrictive rubber band and the Hoffman clamp are able to distribute the tidal volume and inflation pressure appropriately at the airway opening according to the individual lung size. Since both ventilated lung sides are expected to have similar pathologies, the ventilation pattern can be commonly optimized for ARDS by adjusting the PEEP, I:E ratio and FiO_2. Therefore, this model mimics the most important features that allow to address the temporary shortage of ventilators in an emergency situation in COVID-19 patients with pneumonitis-associated ARDS. A fixed ventilation frequency of 12/min and I:E ratio of 1:2 were applied in the present study during the measurements. While alterations in inspiratory and expiratory times may alter the efficiency of the volume shifting maneuver, capnography as a monitoring modality proposed in the present study will reliably indicate the feasibility of this approach. A methodological aspect of the present study is that a simultaneous ventilation may be applied only in controlled mode, since the individual and different spontaneous activity cannot be synchronised neither between the two sides. The use of $ETCO_2$ as a target capnography outcome to control the tidal volume during shared ventilation has further limitation, since this parameter is affected not only by minute volume, but a series of factors affecting intrapulmonary shunt, such as alveolar ventilation, ventilation/perfusion heterogeneity, etc.

5. CONCLUSIONS

In conclusion, our experimental and simulation results support that ventilator sharing can still be considered as a rescue intervention to provide adequate tidal volumes without collateral airflow for two subjects with different respiratory systems. This split ventilation modality can be applied if emergency arise as a result of temporal shortage of mechanical ventilators (Beitler

et al., 2020). However, the responsibility of the health care provider increases in such acute situations, due to the need for additional patient care (Mancebo et al., 2020). Moreover, capnography as a simple, quick and goal-oriented method can serve as a bedside approach to ensure the adequacy of tidal volumes on both lungs during this life saving intervention. This routinely available monitoring modality may help in emergency situations where there is a lack of health care professionals. Ventilator sharing can be regarded as a lifesaving manoeuvre that may be equal to an inevitable triage between patients in catastrophe medicine. This alternative may have importance during the exacerbation of the current or next epidemic wave, when intensive care specialists may be faced with a shortage of ventilators.

DECLARATION OF CONFLICT OF INTEREST

The authors declare to have no potential conflict of interest with respect to the research, authorship, and/or publication of this article.

ACKNOWLEDGMENTS

This work was supported by a Hungarian Basic Research Council Grant (OTKA-NKFIH K115253) and GINOP-2.3.2-15-2016-00006. AS was supported by the New National Excellence Program of the Ministry of Human Capacities of the Hungarian Government (UNKP-19-3). GHF was supported by the National Talent Program by the Hungarian Ministry of Human Capacities (NTP-NFTÖ-19-B-0065).

REFERENCES

Abid, A., Mieloszyk, R.J., Verghese, G.C., Krauss, B.S., Heldt, T., 2017. Model-Based Estimation of Respiratory Parameters from Capnography, With Application to Diagnosing Obstructive Lung Disease. IEEE Trans Biomed Eng 64, 2957-2967.

Babik, B., Petak, F., Asztalos, T., Deak, Z.I., Bogats, G., Hantos, Z., 2002. Components of respiratory resistance monitored in mechanically ventilated patients. Eur Respir J 20, 1538-1544.

Balogh, A.L., Petak, F., Fodor, G.H., Tolnai, J., Csorba, Z., Babik, B., 2016. Capnogram slope and ventilation dead space parameters: comparison of mainstream and sidestream techniques. Br J Anaesth 117, 109-117.

Beitler, J.R., Mittel, A.M., Kallet, R., Kacmarek, R., Hess, D., Branson, R., Olson, M., Garcia, I., Powell, B., Wang, D.S., Hastie, J., Panzer, O., Brodie, D., Hill, L.L., Thompson, B.T., 2020. Ventilator Sharing During an Acute Shortage Caused by the COVID-19 Pandemic. Am J Respir Crit Care Med.

Bhatraju, P.K., Ghassemieh, B.J., Nichols, M., Kim, R., Jerome, K.R., Nalla, A.K., Greninger, A.L., Pipavath, S., Wurfel, M.M., Evans, L., Kritek, P.A., West, T.E., Luks, A., Gerbino, A., Dale, C.R., Goldman, J.D., O'Mahony, S., Mikacenic, C., 2020. Covid-19 in Critically Ill Patients in the Seattle Region - Case Series. N Engl J Med.

Brochard, L., Slutsky, A., Pesenti, A., 2017. Mechanical Ventilation to Minimize Progression of Lung Injury in Acute Respiratory Failure. Am J Respir Crit Care Med 195, 438-442.

Carenzo, L., Costantini, E., Greco, M., Barra, F.L., Rendiniello, V., Mainetti, M., Bui, R., Zanella, A., Grasselli, G., Lagioia, M., Protti, A., Cecconi, M., 2020. Hospital surge capacity in a tertiary emergency referral centre during the COVID-19 outbreak in Italy. Anaesthesia.

Chatburn, R.L., Branson, R.D., Hatipoglu, U., 2020. Multiplex Ventilation: A Simulation-based Study of Ventilating Two Patients with One Ventilator. Respir Care.

Chen, N., Zhou, M., Dong, X., Qu, J., Gong, F., Han, Y., Qiu, Y., Wang, J., Liu, Y., Wei, Y., Xia, J., Yu, T., Zhang, X., Zhang, L., 2020. Epidemiological and clinical characteristics of 99 cases of 2019 novel coronavirus pneumonia in Wuhan, China: a descriptive study. Lancet 395, 507-513.

Clarke, A.L., Stephens, A.F., Liao, S., Byrne, T.J., Gregory, S.D., 2020. Coping with COVID-19: ventilator splitting with differential driving pressures using standard hospital equipment. Anaesthesia.

Csorba, Z., Petak, F., Nevery, K., Tolnai, J., Balogh, A.L., Rarosi, F., Fodor, G.H., Babik, B., 2016. Capnographic Parameters in Ventilated Patients: Correspondence with Airway and Lung Tissue Mechanics. Anesth Analg 122, 1412-1420.

Gattinoni, L., Coppola, S., Cressoni, M., Busana, M., Rossi, S., Chiumello, D., 2020. Covid-19 Does Not Lead to a "Typical" Acute Respiratory Distress Syndrome. Am J Respir Crit Care Med.

Grinnan, D.C., Truwit, J.D., 2005. Clinical review: respiratory mechanics in spontaneous and assisted ventilation. Crit Care 9, 472-484.

Herrmann, J., Fonseca da Cruz, A., Hawley, M.L., Branson, R.D., Kaczka, D.W., 2020. Shared Ventilation in the Era of COVID-19: A Theoretical Consideration of the Dangers and Potential Solutions. Respir Care.

Kheyfets, V.O., Lammers, S.R., Wagner, J., Bartels, K., Piccoli, J., Smith, B.J., 2020. PEEP/ FIO2 ARDSNet Scale Grouping of a Single Ventilator for Two Patients: Modeling Tidal Volume Response. Respir Care 65, 1094-1103.

Lee, C.C.M., Thampi, S., Lewin, B., Lim, T.J.D., Rippin, B., Wong, W.H., Agrawal, R.V., 2020. Battling COVID-19: critical care and peri-operative healthcare resource management strategies in a tertiary academic medical centre in Singapore. Anaesthesia.

Mancebo, J., Richard, J.C., Brochard, L., 2020. Ventilator Sharing during Shortages. A Siren's Song? Am J Respir Crit Care Med 202, 490-491.

Marini, J.J., Gattinoni, L., 2020. Management of COVID-19 Respiratory Distress. JAMA.

Neyman, G., Irvin, C.B., 2006. A single ventilator for multiple simulated patients to meet disaster surge. Acad Emerg Med 13, 1246-1249.

Noble, J., Degesys, N.F., Kwan, E., Grom, E., Brown, C., Fahimi, J., Raven, M., 2020. Emergency department preparation for COVID-19: accelerated care units. Emerg Med J.

Paladino, L., Silverberg, M., Charchaflieh, J.G., Eason, J.K., Wright, B.J., Palamidessi, N., Arquilla, B., Sinert, R., Manoach, S., 2008. Increasing ventilator surge capacity in disasters: ventilation of four adult-human-sized sheep on a single ventilator with a modified circuit. Resuscitation 77, 121-126.

Park, M., Cook, A.R., Lim, J.T., Sun, Y., Dickens, B.L., 2020. A Systematic Review of COVID-19 Epidemiology Based on Current Evidence. J Clin Med 9.

Phua, J., Weng, L., Ling, L., Egi, M., Lim, C.M., Divatia, J.V., Shrestha, B.R., Arabi, Y.M., Ng, J., Gomersall, C.D., Nishimura, M., Koh, Y., Du, B., Asian Critical Care Clinical Trials, G., 2020. Intensive care management of coronavirus disease 2019 (COVID-19): challenges and recommendations. Lancet Respir Med.

Sanche, S., Lin, Y.T., Xu, C., Romero-Severson, E., Hengartner, N., Ke, R., 2020. High Contagiousness and Rapid Spread of Severe Acute Respiratory Syndrome Coronavirus 2. Emerg Infect Dis 26.

Shovlin, C.L., Vizcaychipi, M.P., 2020. Implications for COVID-19 triage from the ICNARC report of 2204 COVID-19 cases managed in UK adult intensive care units. Emerg Med J 37, 332-333.

Wax, R.S., Christian, M.D., 2020. Practical recommendations for critical care and anesthesiology teams caring for novel coronavirus (2019-nCoV) patients. Can J Anaesth 67, 568-576.

Wilcox, S.R., 2020. Management of respiratory failure due to covid-19. BMJ 369, m1786.

Xie, J., Tong, Z., Guan, X., Du, B., Qiu, H., Slutsky, A.S., 2020. Critical care crisis and some recommendations during the COVID-19 epidemic in China. Intensive Care Med.

Zhou, F., Yu, T., Du, R., Fan, G., Liu, Y., Liu, Z., Xiang, J., Wang, Y., Song, B., Gu, X., Guan, L., Wei, Y., Li, H., Wu, X., Xu, J., Tu, S., Zhang, Y., Chen, H., Cao, B., 2020. Clinical course and risk factors for mortality of adult inpatients with COVID-19 in Wuhan, China: a retrospective cohort study. Lancet 395, 1054-1062.

FIGURE LEGENDS

Figure 1. Scheme of the experimental setup. The inspiratory and expiratory limbs connected to the ventilator were divided into two symmetrical pathways. Both inspiratory and expiratory tubing were connected after the inspiratory and before the expiratory valves of the respirator, respectively. Two identical systems were used to measure CO_2 concentration, pressure was measured by using pressure transducers via lateral ports ("Transducer (Pressure)"), and airflow was sensed by calibrated screen pneumothachographs ("PTG (Airflow)") in each artificial lung. The controlled CO_2 inflow into each model lung side was standardized by using a flow generator connected via tubing equipped with CO_2 clamps. Only one of the CO_2 clamps was open during the capnography measurements to avoid uneven distribution of CO_2 flow into each lung side depending on the load impedance. The model lung with red rubber band represents low compliance side, while the model lung with blue Hoffman clamp denotes the increased resistance. Lung HR: high resistance lung side, Lung LC: low-compliance lung side.

Figure 2. Representative volume, capnogram (PCO_2), airflow and pressure curves obtained under baseline condition (left panels), during unilateral decreased compliance (middle panels) and following the compensation of unilaterally decreased compliance with contralateral high resistance (right panels) during volume-controlled ventilation. Black curves represent no intervention, red curves reflect low compliance side (Low C), blue curves denote high resistance side (High R).

Figure 3. Tidal volume (VT), end-tidal CO_2 concentration ($ETCO_2$), peak inspiratory- (PIP) and expiratory flows (PEF) and peak inspiratory pressure (Ppi) obtained by averaging the 30-s long recordings under volume- (left) and pressure-controlled (right) ventilations. Black bars represent no intervention, red curves reflect low compliance side (Low C), blue curves denote high resistance side (High R). Results were obtained under baseline conditions (BL), after

unilateral decrease in compliance (LC) and contralateral compensation with high resistance (LC + HR).

Figure 4. Panel A: The shared ventilation system is modeled by parallel connection of single compartment respiratory system impedances including resistance and compliance. **Panel B**: equation to calculate the compensatory resistance to equalize different impedances. Results of the mathematical simulation study with setting physiological (**Panel C**) and moderately elevated (**Panel D**) total respiratory resistance levels on the low-compliance side (R_{LC}). The nomograms with different curves show the resistance values necessary to counterbalance the asymmetry in compliance values to deliver the same tidal volumes to both sides of a split ventilation circuit. The compliance values of the two ventilated sides are indicated on the labelled curves (C_{HR}) and the x-axis (C_{LC}), respectively. The targeted contralateral resistance values are obtained from the y-axis. Red arrows indicate a particular example: a resistance value of 14.9 $cmH_2O.s/l$ (R_{HR}) is necessary to counterbalance the compliance asymmetry if the resistance and compliance on the low compliance side is 8 $cmH_2O.s/l$ (R_{LC}) and 40 ml/cmH_2O (C_{LC}), respectively, and the compliance on the contralateral side is 55 ml/cmH_2O (C_{HR}).

		R_{LC}	R_{HR}	R	C_{LC}	C_{HR}	C	τ_{LC}	τ_{HR}
VC	**BL**	*17.4*	*17.4*	8.7	*33*	*33*	65	*0.57*	*0.57*
	LC	*18.2*	*18.2*	9.1	*20*	*34*	54	*0.36*	*0.63*
	LC + HR	*17.4*	*40.7*	12.2	*18*	*31*	49	*0.31*	*1.27*
PC	**BL**	*17.4*	*17.4*	8.7	*33*	*33*	65	*0.57*	*0.57*
	LC	*18.2*	*18.2*	9.1	*20*	*35*	55	*0.36*	*0.64*
	LC + HR	*17.4*	*39.5*	12.1	*18*	*33*	51	*0.32*	*1.28*

Table 1. Resistance, compliance parameters displayed by the ventilator (R and C) and time constant ($\tau = R \cdot C$) under baseline conditions (BL), after unilateral decrease in compliance (LC) and contralateral compensation with high resistance (LC + HR) in volume- (VC) and pressure-controlled (PC) ventilation modes. Calculation of individual compliance values were based on the measured tidal volumes and distending pressures on each side. Calculation of individual resistances are based on equation (4) by assuming parallel arrangement of the individual tubing. R and C values are expressed in $cmH_2O.s/l$ and ml/cmH_2O, respectively. τ is in seconds. Normal fonts: measured parameters, italic fonts: calculated parameters. Indices "LC" and "HR" indicate resistance, compliance and time constant parameters on the low-compliance and high-resistance sides, respectively.

Figure 1

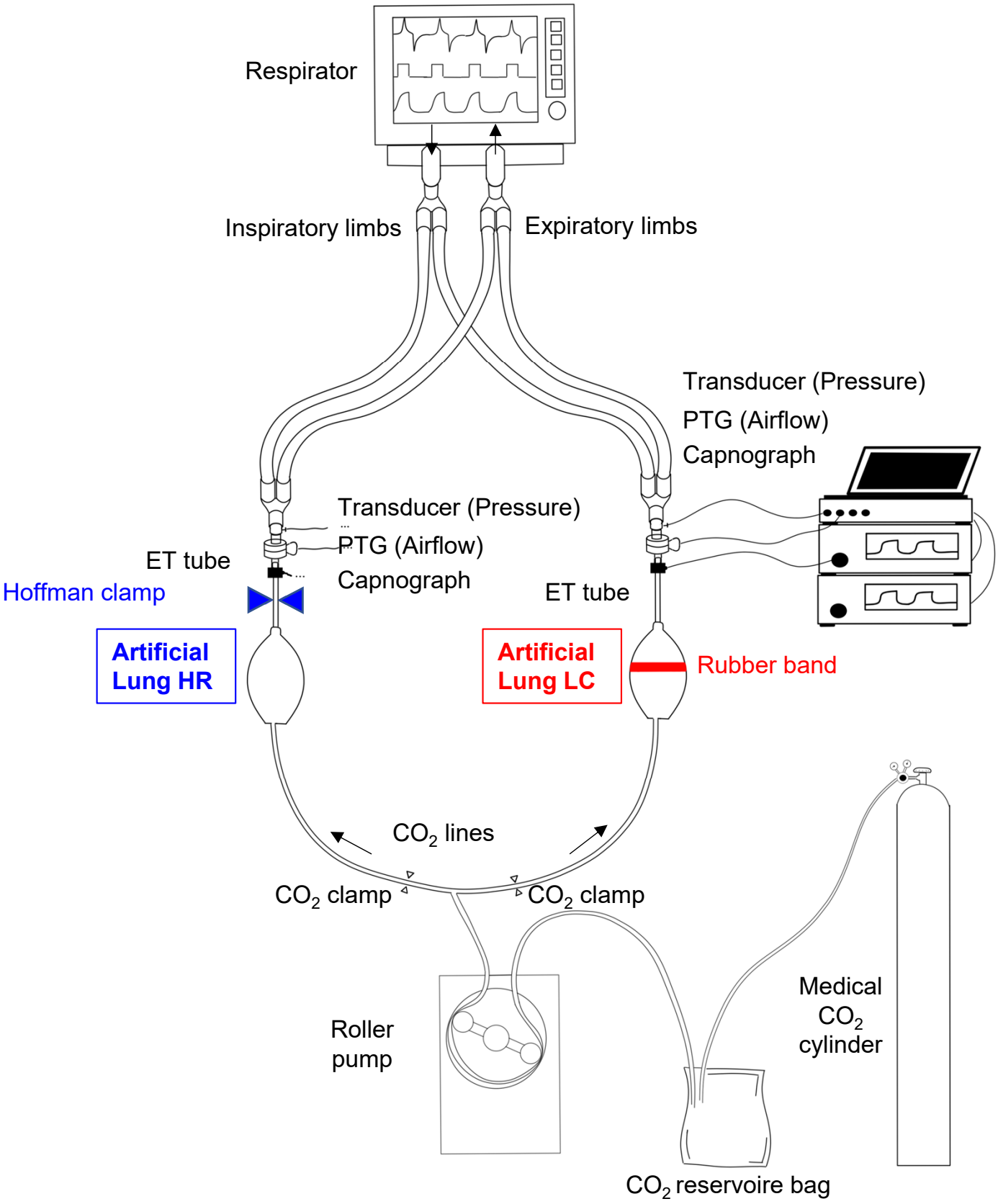

Figure 1.

Figure 2

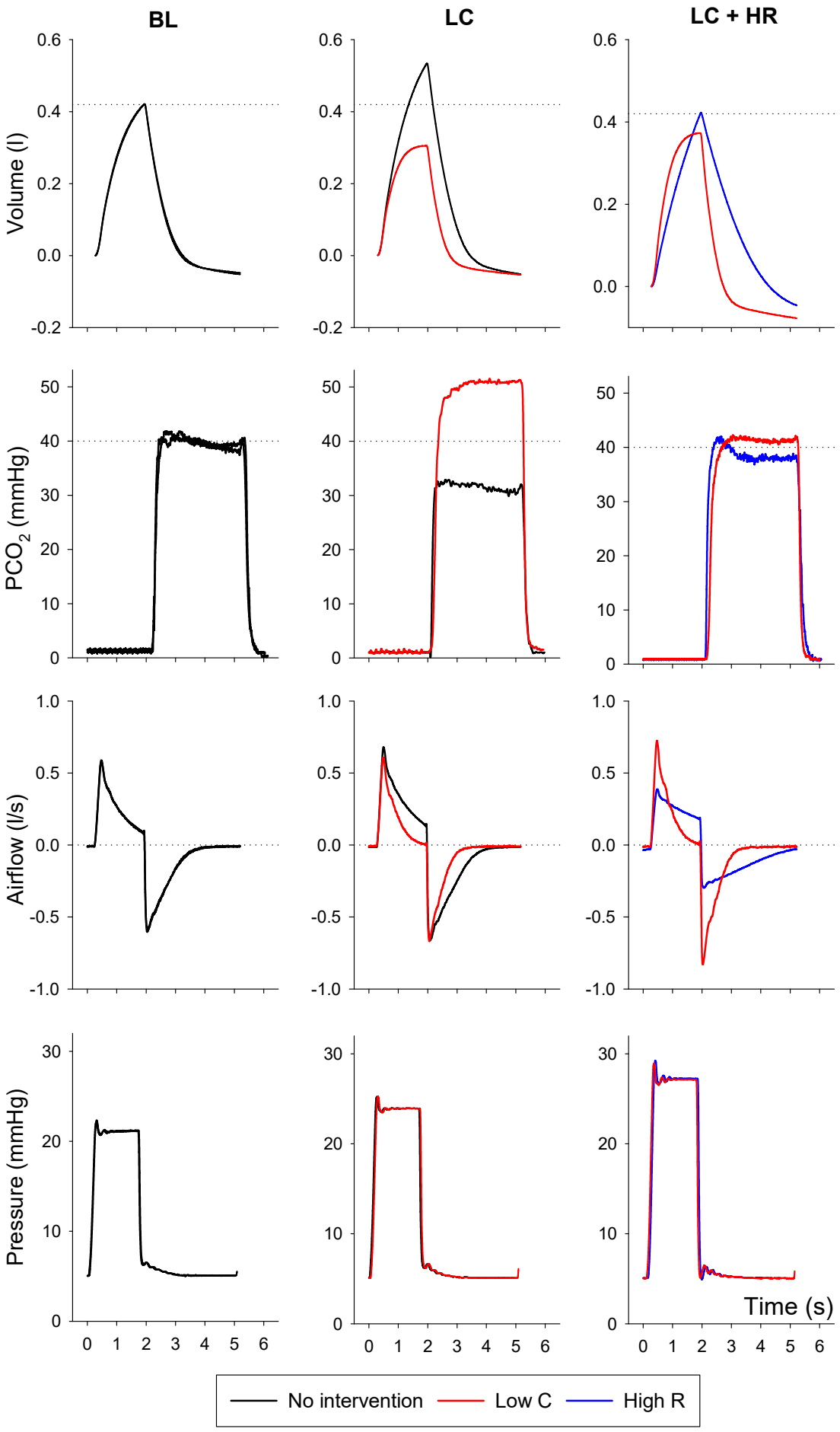

Figure 2

Figure 3

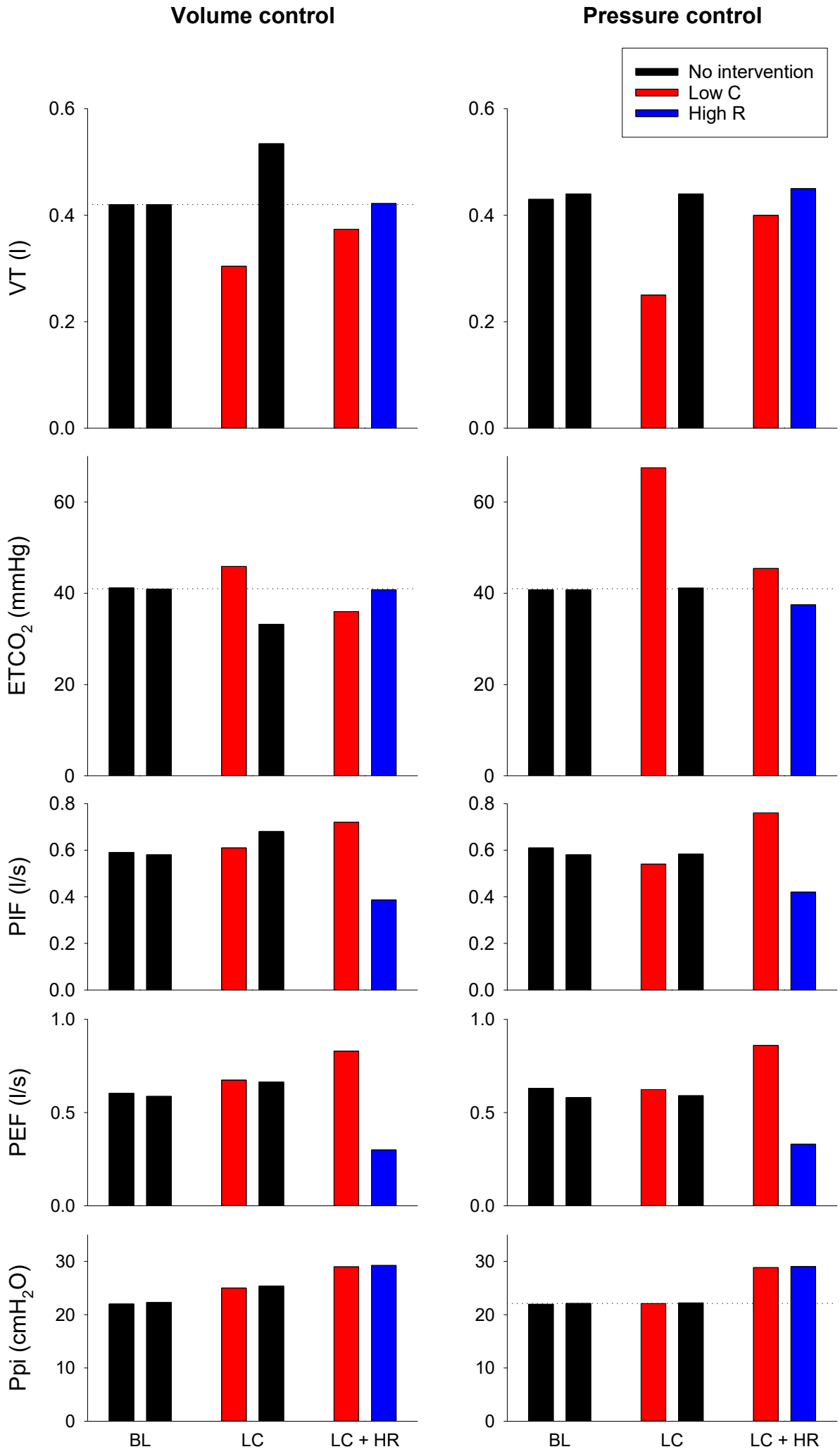

Figure 3

Figure

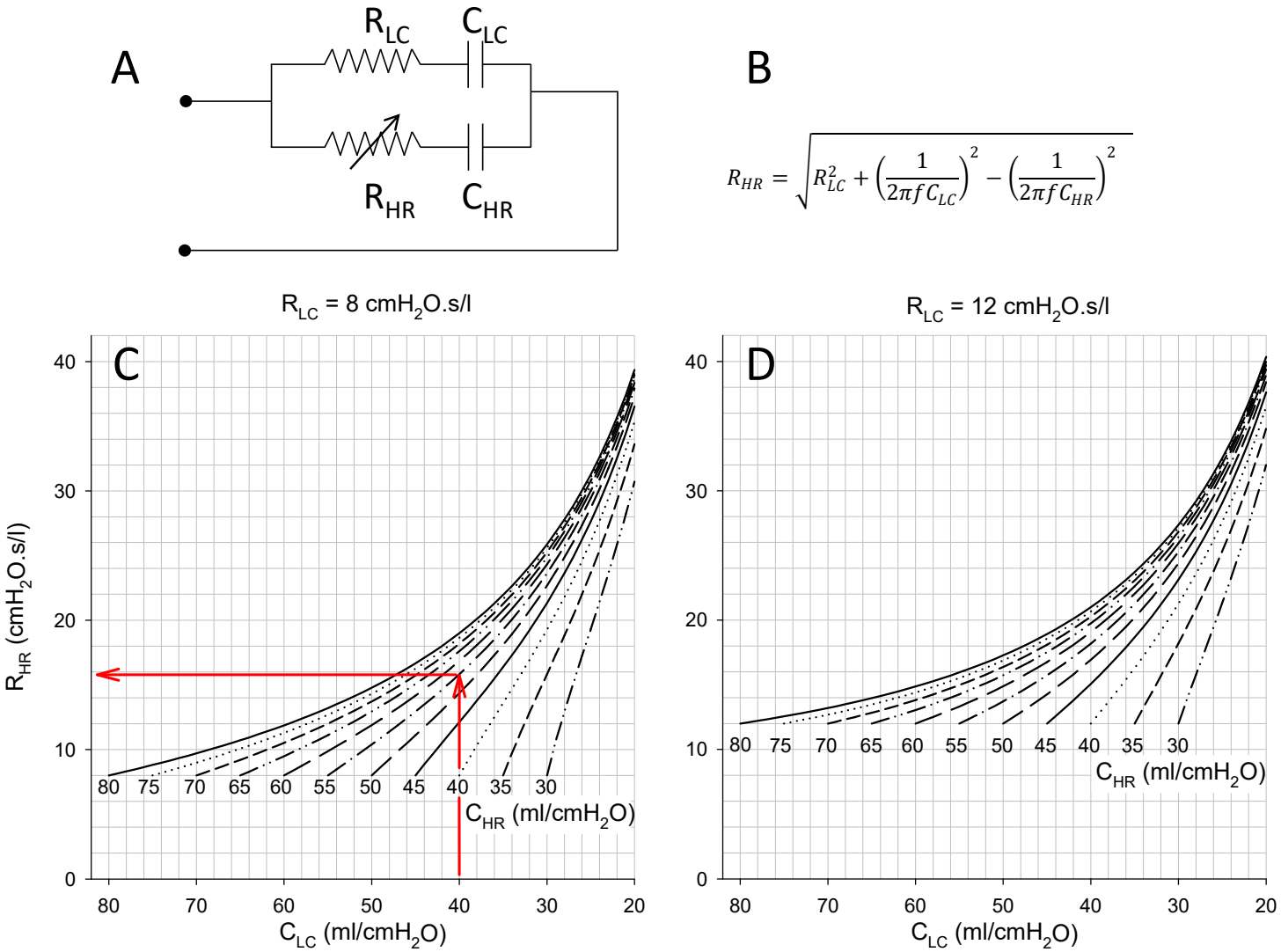

Figure 4